

Performance Analysis of Energy Harvesting Multi-Antenna Relay Networks With Different Antenna Selection Schemes

YUZHEN HUANG^{1,2}, (Member, IEEE), JINLONG WANG², (Senior Member, IEEE),
PING ZHANG¹, (Senior Member, IEEE), AND QIHUI WU³, (Senior Member, IEEE)

¹School of Information and Communication, Beijing University of Posts and Telecommunications, Beijing 100876, China

²College of Communications Engineering, Army Engineering University of PLA, Nanjing 210007, China

³College of Electronic and Information Engineering, Nanjing University of Aeronautics and Astronautics, Nanjing 210016, China

Corresponding author: Yuzhen Huang (yzh_huang@sina.com)

This work was supported in part by the National Science Foundation of China under Grant 61501507, in part by the Jiangsu Provincial Natural Science Foundation of China under Grant BK20150719, and in part by the China Postdoctoral Science Foundation Funded Project under Grant 2017M610066.

ABSTRACT In this paper, we investigate the performance of three transmit antenna selection (TAS) schemes for an energy harvesting decode-and-forward relay cooperative network. In the network, the energy-limited relay first harvests the energy from the received signal with the power-splitting scheme, and then utilizes the harvested energy to forward the received signal to the destination. Specifically, exact analytical expressions for the outage probability of the considered network with three TAS schemes are derived for evaluating the impact of key parameters on the outage performance. In order to deeply extract insights, we further present tractable asymptotic outage probabilities for three TAS schemes to characterize the diversity order and coding gain in high signal-to-noise ratio regimes, respectively. In addition, we also analyze the impact of feedback delays on the performance of the optimal TAS scheme, which is quantified by the reduction of diversity order and coding gain. Numerical results sustained by Monte Carlo simulations demonstrate that: 1) the second suboptimal TAS schemes achieve a comparable performance as the optimal TAS scheme with the reduced implementation cost; 2) the relay location has a great impact on the outage performance and the optimal power-splitting ratio; and 3) the feedback delay plays a critical role in determining the diversity order achieved by the considered system.

INDEX TERMS Energy harvesting, decode-and-forward (DF) relaying, cooperative relay network, transmit antenna selection (TAS), outage probability.

I. INTRODUCTION

The swift proliferation of wireless multimedia applications coupled with ever growing number of online games has dried up the energy of conventional wireless communication systems. As such, in order to maintain the network connectivity, wireless networks or wireless devices need to be frequently plugged into the power grid for recharging, which greatly affects the user experience. Specifically, in the next generation mobile communication system, i.e., 5G, compared to 4G, the Quality of Experience perceived by users will be greatly improved, such as spectral efficiency and energy efficiency. That is, we need to look for new techniques to prolong the lifetime of energy-constrained wireless networks or wireless devices. In this context, energy harvesting techniques,

which can scavenge energy from the external resources, such as solar power, wind energy, piezoelectric and geothermal effects, were proposed in [1] and [2]. However, the limitation of these techniques is that the external resources, e.g., wind and solar, are the inherent randomness and highly dependent on the weather conditions. Inspired by this important observation, radio-frequency (RF) signals-based energy harvesting techniques, as a part of wireless communication networks, have drawn considerable attention from the academia and industry alike [3], [4]. That is to say, an RF signal not only can carry the information, but also transfer the wireless energy, which facilitates a new energy harvesting technology, i.e., *simultaneous wireless information and power transfer* (SWIPT).

A. LITERATURE

The fundamental performance limitation as well as efficient design in SWIPT systems with various scenarios are broadly investigated in many prior works. In two seminal works [5] and [6], the tradeoff between the harvested energy and the achievable rate were investigated, respectively. Unfortunately, in [6], the authors assumed an impractical receiver circuit, which can decode the information and harvest energy from the same signal simultaneously. Later, two practical energy harvesting receiver architectures, namely time-switching receiver and power-splitting receiver, were proposed in a point-to-point wireless link [7]. Since then, a number of works have investigated different aspects of simultaneous information and energy transfer with practical receivers [8]–[10]. Specifically, in [8], wireless information and power transfer was first investigated in a co-channel interference environment, and various tradeoffs, i.e., so-called “outage-energy” region and “rate-energy” region, were analyzed to achieve the optimal energy harvesting mode at receiver. In [9], a dedicated power beacon was deployed to power the energy-limited information source, and then the average throughput of delay tolerant and intolerant transmission modes was analyzed, respectively. Later, a dynamic power-splitting receiver, where the received signal was split into two streams based on the instantaneous channel condition, was proposed in [10] to improve the system performance.

Recently, since multi-antenna techniques can fully achieve the spatial diversity and spatial multiplexing, RF energy transfer in the context of multi-antenna systems has been broadly investigated in [11]–[18]. Specifically, in order to maximize the efficiency of simultaneous information and energy transmission, some fundamental tradeoffs in designing multiple-input multiple-output (MIMO) systems were discussed in [14]. Furthermore, the authors in [15] considered a multiuser multiple-input single output (MISO) interference channel, where the receivers are characterized by both quality-of-service (QoS) and RF energy harvesting constraints. In [16], the average throughput performance of energy beamforming in multi-antenna wireless-powered communication networks was investigated in both two transmission modes, respectively. In addition, [17] investigated the optimal transmit beamforming designs for SWIPT in MISO interference channels. Finally, in [18], the achievable throughput of wireless energy transfer enabled massive MIMO systems was investigated under the condition of imperfect channel state information (CSI).

On the other hand, the applications of RF energy harvesting technique on cooperative relaying networks are also interesting, which have been received much attention. For example, in [19], two relaying protocols, i.e., time-switching based relaying protocol and power-splitting based relaying protocol, were proposed to enable wireless energy harvesting and information processing at the relay. Later, in [20], two novel time-switching based protocols for continuous

time and discrete time energy harvesting were proposed in amplify-and-forward (AF) and decode-and-forward (DF) relaying networks, respectively. In the co-channel interference scenario, [21] analyzed the ergodic capacity and the outage capacity of RF-based energy harvesting relaying networks with the time-switching and power-splitting protocols, respectively. Given a energy transfer constraint, [22] proposed a relay selection policy to achieve the optimal tradeoff in a maximum capacity/minimum outage probability sense. In [23], the authors analyzed the effects of line-of-sight and opportunistic scheduling on dual-hop energy harvesting relay systems. In addition, the authors in [24] exploited the direct links in multiuser multirelay SWIPT cooperative networks to improving the outage performance. Afterwards, in order to take advantage of both multi-antenna and cooperative relaying techniques, some recent works have investigated the performance of RF-based energy harvesting multi-antenna relaying networks in [25]–[27]. Specifically, in [25], three different linear processing schemes were proposed to exploit the benefits of multiple antennas in an energy harvesting relaying system with/without co-channel interference environment. To reduce the implementation complexity and power requirement at the transmitter, [26] proposed a joint antenna selection and power-splitting technique to maximize the achievable rate of energy harvesting relay networks. In [27], the authors designed a joint relay-and-antenna selection scheme in energy harvesting MIMO DF relay cooperative networks to minimize the outage performance. While in [28], the authors designed optimal and suboptimal linear processing schemes in wireless-powered multi-antenna full-duplex relaying systems with the time-switching protocol. Furthermore, in [29], the authors proposed the hop-by-hop information and energy beamforming for wireless powered MIMO relaying systems in the presence of interference at the destination.

B. MOTIVATION AND CONTRIBUTIONS

Different from above all discussed works, in this paper, we focus on investigating the outage performance of an energy harvesting DF relay network with multiple antennas over independent and non-identical Rayleigh fading, taking into account the direct link between the source and destination. In the network, the energy-constrained relay collects the energy from RF signals with the power-splitting protocol, and utilizes the harvested energy to forward the information to the destination when the relay link is selected. Specifically, to reduce the implementation complexity of the system, we design an optimal and two suboptimal TAS schemes at the source for the considered network based on the availability of link CSIs. Moreover, the impact of outdated CSI due to feedback delay on the outage performance of the considered system with optimal TAS scheme is also analyzed. The main contributions of our paper are summarized as follows:

- For all TAS schemes, we derive the exact analytical expressions of the outage probability for the considered system with the power-splitting protocol. The derived

results provide an efficient means to evaluate the impact of key parameters on the system performance and allow us to avoid the time-consuming Monte Carlo simulations. In addition, we also provide the exact outage probability expression to quantify the impact of outdated CSI on the outage performance of the considered system with optimal TAS scheme.

- In order to achieve the insights on the design and application of the considered system, we provide the asymptotic outage expressions of all TAS schemes in high SNR regimes. These asymptotic outage expressions easily enable us to obtain the diversity order and coding gain. The analytical results show that three TAS schemes achieve the same diversity order as the conventional relay networks with fixed power supplying. Moreover, we also characterize the diversity order and coding gain achieved by the considered system with optimal TAS scheme in the presence of feedback delay.
- All analytical results are validated by exhaustive Monte Carlo simulations. The impacts of the system parameters, such as antenna number, power-splitting factor, relay location and feedback delay on the outage performance of the considered system are extensively investigated. Numerical results demonstrate that the second suboptimal TAS schemes achieve a similar performance as the optimal TAS scheme with lower implementation complexity. Moreover, feedback delay produces a negative impact on the diversity order, that is when there exists feedback delay, the transmit diversity of the considered system will be reduced to zero.

C. STRUCTURE AND NOTATIONS

The paper is organized as follows. The system model is described in Section II. Section III introduces the three antenna selection schemes. In Section IV, the key performance analysis is provided. In Section V, we present numerical results and discussions. Finally, Section VI concludes the paper and summarizes the findings.

Notations: We use bold lower case letters to denote vectors and lower case letters to denote scalars, respectively. The probability density function (PDF) and the cumulative distribution function (CDF) of a random variable (RV) X are denoted as $f_X(\cdot)$ and $F_X(\cdot)$, respectively. $(\cdot)^T$ denotes the transpose operator and $\|\cdot\|_F$ denotes the Frobenius norm.

II. SYSTEM MODEL

Let us consider an energy harvesting dual-hop DF relay network as shown in Fig. 1, which consists of a source (S) equipped with N_s antennas, an energy-constrained relay (R) equipped with single antenna and a destination (D) equipped with N_d antennas, respectively. Notably, the considered system is of practical importance (e.g. multi-antenna access points communicating via a single antenna mobile relay in wireless networks [30]), which is also considered in [31]–[33]. In this paper, the following assumptions are adopted: a) We assume that all the

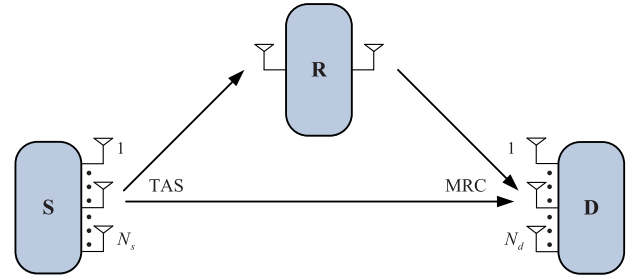


FIGURE 1. System model.

terminals operate in half-duplex mode, and the direct link between the source and the destination is available. b) All channels are modeled as quasi-static block flat fading and remain constant over the block time, and varies independently and identically from one block to another. c) As in [34], full CSIs of links $S \rightarrow R$ and $S \rightarrow D$ are available at S , which can be obtained through the traditional channel estimation. d) The relay first harvests the energy from the received source signal, and then forwards the source signal to the destination with the harvested energy when the relay link is selected. Without loss of generality, we assume that the $N_s \times 1$ channel vector between S and R is denoted by $\mathbf{h}_{SR} = [h_{1,1}, \dots, h_{1,i}, \dots, h_{1,N_s}]^T$, and its entries follow i.i.d. complex Gaussian distribution with zero-mean and variance Ω_1 . The $N_d \times 1$ channel vector between R and D is denoted by $\mathbf{h}_{RD} = [h_{2,1}, \dots, h_{2,n}, \dots, h_{2,N_d}]^T$, each entry of which follows i.i.d. complex Gaussian distribution with zero-mean and variance Ω_2 . In addition, the $N_d \times N_s$ channel matrix between S and D is denoted by $\mathbf{H}_{SD} = [\mathbf{h}_{0,1}, \dots, \mathbf{h}_{0,k}, \dots, \mathbf{h}_{0,N_s}]$, each entry in which follows complex Gaussian distribution with zero-mean and variance Ω_0 .

Since each node in this network is operated in a half-duplex mode, the total transmission consists of two consecutive time slots. During the first phase, the signal x is broadcasted by S with the selected antenna, while D employs the maximal ratio combining (MRC) reception scheme to detect the received signal. For example, when the i -th antenna at S is selected to transmit, hence, the received signals at R and D are respectively expressed as

$$y_R = \sqrt{P_s} h_{1,i} x + n_R, \tag{1}$$

and

$$y_D = \sqrt{P_s} \mathbf{h}_{0,i} x + \mathbf{n}_D, \tag{2}$$

where P_s is the transmit power at S , n_R is the additive white Gaussian noise with variance σ^2 at R , and \mathbf{n}_D is the additive noise vector with variance σ^2 at D , respectively. Since the relay is an energy-constrained node, hence, the relay will first replenish the energy from the received signal. As in [24], we focus on the power-splitting protocol in this paper.¹ Hence, at the end of the first phase, the relay splits the

¹Please note, we only consider the power-splitting scheme at the relay to harvest the energy from the received signal, however, the analysis of this paper can be easily extended to the time-splitting scheme.

received signal into two streams, one for energy harvesting and the other for information processing. As indicated in [10], [22], and [35], the harvested power at the relay is given by

$$P_r = \alpha \eta P_s |h_{1,i}|^2, \quad (3)$$

where α ($0 < \alpha < 1$) denotes the power-splitting ratio and η ($0 < \eta < 1$) is the energy conversion efficiency. Hence, the instantaneous signal-to-noise ratio (SNR) between the i -th antenna at S and R can be derived as

$$\gamma_{1,i} = (1 - \alpha) \frac{P_s}{\sigma^2} |h_{1,i}|^2. \quad (4)$$

Similarly, the instantaneous SNR between the i -th antenna at S and D during the first phase can be expressed as

$$\gamma_{0,i} = \frac{P_s}{\sigma^2} \|\mathbf{h}_{0,i}\|_F^2. \quad (5)$$

In the second phase, R first decodes the received source signal, and then forwards the detected symbol with the harvested energy. Similarly, adopting MRC reception at D , the instantaneous SNR between R and D during the second phase is given by

$$\gamma_{2,i} = \alpha \eta \frac{P_s}{\sigma^2} |h_{1,i}|^2 \|\mathbf{h}_{RD}\|_F^2. \quad (6)$$

Similar to [24] and [36], we adopt the fixed DF protocol at relay. Thus, when the i -th antenna at S is selected, the instantaneous SNR of relaying link can be expressed as

$$\gamma_{SR,i} = \min(\gamma_{1,i}, \gamma_{2,i}). \quad (7)$$

Finally, to reduce the implementation cost of the system, we adopt the selection combining technique at D to combine the direct signal and the relaying signal as in [37] and [38]. Thus, the instantaneous end-to-end SNR of the system with the i -th antenna selected at S is derived as

$$\gamma_{e,i} = \max(\gamma_{0,i}, \gamma_{SR,i}). \quad (8)$$

III. TRANSMIT ANTENNA SELECTION SCHEMES

Now, in the following section, we will take our attention to the proposed three TAS schemes for the energy harvesting DF relay networks based on the availability of link CSIs.

A. OPTIMAL TAS SCHEME

When the full CSIs of links $S \rightarrow D$ and $S \rightarrow R$ are available at the center control unit (for example, it may be S or D), the optimal antenna at S is selected by maximizing $\gamma_{e,i}$ as follows:

$$i^* = \arg \max_{1 \leq i \leq N_s} (\gamma_{e,i}). \quad (9)$$

where i^* is the optimal antenna index at S .

B. SUBOPTIMAL TAS SCHEME

As discussed in the optimal TAS scheme, we find that it requires the full CSIs of $S \rightarrow D$ and $S \rightarrow R$ links, which results in a higher implementation cost and the amount of CSIs feedback. To address with this, similar to [39] we

propose two suboptimal TAS schemes for energy harvesting MIMO DF relay networks based on the partial CSIs.

- 1) **Suboptimal TAS₁**: In this suboptimal scheme, the antenna at S is selected to maximize the SNR of link $S \rightarrow R$. Hence, the selected antenna index is expressed as

$$i^* = \arg \max_{1 \leq i \leq N_s} (\gamma_{1,i}). \quad (10)$$

From the above equation, we can see that the antenna selected at S only depends on the CSI of link $S \rightarrow R$.

- 2) **Suboptimal TAS₂**: In this suboptimal scheme, the antenna at S is selected to maximize the SNR of link $S \rightarrow D$. Hence, the selected antenna index is given as

$$i^* = \arg \max_{1 \leq i \leq N_s} (\gamma_{0,i}). \quad (11)$$

As indicated in this equation, only CSI of link $S \rightarrow D$ is needed to select the antenna at S .

Now, in the following section, we will focus on analyzing the key performance of energy harvesting DF relay networks with the three TAS schemes, respectively.

IV. OUTAGE PERFORMANCE ANALYSIS

In this section, we turn our attention to evaluate the performance of energy-harvesting DF relay networks with three TAS schemes in terms of outage probability. The outage probability is an important performance metric, which is appropriate for evaluating the delay intolerant services, e.g., voice and video. Mathematically, it is defined as the instantaneous end-to-end SNR falls below a given outage threshold γ_{th} , i.e.,

$$P_{out}(\gamma_{th}) = \Pr(\gamma_{e,i^*} < \gamma_{th}), \quad (12)$$

where $\gamma_{th} = 2^{2R_0} - 1$ with R_0 being the target data rate.

A. OPTIMAL TAS SCHEME

From (8) and (9), the outage probability achieved by the optimal TAS scheme can be formulated as

$$P_{out}^{opt}(\gamma_{th}) = \Pr\left(\max_{1 \leq i \leq N_s} \max\{\gamma_{0,i}, \min\{\gamma_{1,i}, \gamma_{2,i}\}\} < \gamma_{th}\right). \quad (13)$$

Theorem 1: The exact analytical expression for outage probability of energy harvesting DF relay networks with the optimal TAS scheme can be derived as

$$P_{out}^{opt}(\gamma_{th}) = \left[1 - \frac{1}{\Gamma(N_d)} \Gamma\left(N_d, \frac{\gamma_{th}}{\bar{\gamma}_0}\right)\right]^{N_s} \left[1 - \frac{N_s}{1 - \alpha} \times \frac{\gamma_{th}}{\bar{\gamma}_1} \sum_{n=0}^{N_s-1} \binom{N_s-1}{n} \sum_{m=0}^{N_d-1} \sum_{k=0}^{\infty} \frac{(-1)^{k+n}}{m!k!} \times \left(\frac{1 - \alpha}{\alpha \eta \Omega_2}\right)^{m+k} E_{m+k}\left(\frac{\gamma_{th}(n+1)}{(1 - \alpha)\bar{\gamma}_1}\right)\right], \quad (14)$$

where $\Gamma(\cdot)$ is the Gamma function [40, eq. (8.310)], $\Gamma(\cdot, \cdot)$ is the upper incomplete Gamma function [40, eq. (8.350.2)],

$$\begin{aligned}
 P_{\text{out}}^{\text{opt}}(\gamma_{\text{th}}) & \approx \begin{cases} \frac{1}{(N_d!)^{N_s}} \left(\frac{\gamma_{\text{th}}}{\bar{\gamma}_0}\right)^{N_s N_d} \left(\frac{\gamma_{\text{th}}}{(1-\alpha)\bar{\gamma}_1}\right)^{N_s} \left[1 + \sum_{n=0}^{N_s-1} \binom{N_s-1}{n} \frac{(-1)^{n+N_s} (n+1)^{N_s-1}}{N_s^{-1} \Gamma(N_d) \Gamma(N_s)} \sum_{k=0}^{\infty} \frac{(-1)^{k+1} \vartheta^{N_d+k}}{k! (N_d+k)} \frac{1}{(N_d-N_s+k)} \right], & N_s < N_d \\ \frac{1}{(N_d!)^{N_s}} \left(\frac{\gamma_{\text{th}}}{\bar{\gamma}_0}\right)^{N_s N_d} \left(\frac{\gamma_{\text{th}}}{(1-\alpha)\bar{\gamma}_1}\right)^{N_s} \left\{ 1 + \sum_{n=0}^{N_s-1} \binom{N_s-1}{n} \frac{(-1)^{n+N_s} (n+1)^{N_s-1}}{\vartheta^{-N_s} \Gamma(N_d) \Gamma(N_s)} \left[\ln(\varpi) - \psi(N_s) + \sum_{k=1}^{\infty} \frac{N_s (-1)^{k-1} \vartheta^k}{k! (N_s+k) k} \right] \right\}, & N_s = N_d \\ \frac{1}{(N_d!)^{N_s}} \left(\frac{\gamma_{\text{th}}}{\bar{\gamma}_0}\right)^{N_s N_d} \left(\frac{\gamma_{\text{th}}}{(1-\alpha)\bar{\gamma}_1}\right)^{N_d} \sum_{n=0}^{N_s-1} \binom{N_s-1}{n} \frac{N_s (-1)^{n+N_d} (n+1)^{N_d-1}}{\vartheta^{-N_d} \Gamma(N_d+1) \Gamma(N_d)} [\ln(\varpi) - \psi(N_d)], & N_s > N_d \end{cases} \quad (15)
 \end{aligned}$$

$$\begin{aligned}
 P_{\text{out}}^{\text{sub1}}(\gamma_{\text{th}}) & \approx \begin{cases} \frac{1}{N_d!} \left(\frac{\gamma_{\text{th}}}{\bar{\gamma}_0}\right)^{N_d} \left(\frac{\gamma_{\text{th}}}{(1-\alpha)\bar{\gamma}_1}\right)^{N_s} \left[1 + \sum_{n=0}^{N_s-1} \binom{N_s-1}{n} \frac{(-1)^{n+N_s} (n+1)^{N_s-1}}{N_s^{-1} \Gamma(N_d) \Gamma(N_s)} \sum_{k=0}^{\infty} \frac{(-1)^{k+1} \vartheta^{N_d+k}}{k! (N_d+k)} \frac{1}{(N_d-N_s+k)} \right], & N_s < N_d \\ \frac{1}{N_d!} \left(\frac{\gamma_{\text{th}}}{\bar{\gamma}_0}\right)^{N_d} \left(\frac{\gamma_{\text{th}}}{(1-\alpha)\bar{\gamma}_1}\right)^{N_s} \left\{ 1 + \sum_{n=0}^{N_s-1} \binom{N_s-1}{n} \frac{(-1)^{n+N_s} (n+1)^{N_s-1}}{\vartheta^{-N_s} \Gamma(N_d) \Gamma(N_s)} \left[\ln(\varpi) - \psi(N_s) + \sum_{k=1}^{\infty} \frac{N_s (-1)^{k-1} \vartheta^k}{k! (N_s+k) k} \right] \right\}, & N_s = N_d \\ \frac{1}{N_d!} \left(\frac{\gamma_{\text{th}}}{\bar{\gamma}_0}\right)^{N_d} \left(\frac{\gamma_{\text{th}}}{(1-\alpha)\bar{\gamma}_1}\right)^{N_d} \sum_{n=0}^{N_s-1} \binom{N_s-1}{n} \frac{N_s (-1)^{n+N_d} (n+1)^{N_d-1}}{\vartheta^{-N_d} \Gamma(N_d+1) \Gamma(N_d)} [\ln(\varpi) - \psi(N_d)], & N_s > N_d \end{cases} \quad (18)
 \end{aligned}$$

$E_n(\cdot)$ is the Exponential integrals function [41, eq. (5.1.4)], $\bar{\gamma}_0 = \frac{P_s \Omega_0}{\sigma^2}$, and $\bar{\gamma}_1 = \frac{P_s \Omega_1}{\sigma^2}$.

Proof: See Appendix A. ■

The derived analytical result in Theorem 1 provides an efficient way to evaluate the outage performance of the considered system with the optimal TAS scheme, however, it is in general too complex to achieve further insight. Motivated by this, we now look into the high SNR regime, i.e., $\bar{\gamma} = \frac{P_s}{\sigma^2} \rightarrow \infty$, and present an asymptotic analysis of outage probability, which easily enable us to achieve the diversity order and coding gain.

Corollary 1: In the high SNR regime, i.e., $\bar{\gamma} \rightarrow \infty$, the outage probability of energy harvesting DF relay networks with the optimal TAS scheme can be approximated as (15), as shown at the top of this page, where $\vartheta = \frac{1-\alpha}{\alpha \eta \Omega_2}$, $\varpi = \frac{\gamma_{\text{th}}(n+1)}{(1-\alpha)\bar{\gamma}_1}$, and $\psi(\cdot)$ is the Digamma function [40, eq. (8.360.1)].

Proof: See Appendix B. ■

Remark 1: From (15), we find that the achievable diversity order of energy harvesting DF relay networks with the optimal TAS scheme is the same as that of traditional MIMO DF relay networks, which demonstrates that the power-splitting ratio has no impact on the diversity order. However, the power-splitting ratio affects the outage performance of the considered system through the coding gain.

B. SUBOPTIMAL TAS₁ SCHEME

In the first suboptimal TAS scheme, the antenna at S is only selected based on the CSI of link $S \rightarrow R$. That is to say, it corresponds to a random antenna selection for link $S \rightarrow D$. Hence, according to (8) and (10), the outage probability achieved by this suboptimal TAS scheme can be formulated as

$$P_{\text{out}}^{\text{sub1}}(\gamma_{\text{th}}) = \Pr(\gamma_{0,i^*} < \gamma_{\text{th}}) \Pr\left(\max_{1 \leq i \leq N_s} \gamma_{\text{SR},i} < \gamma_{\text{th}}\right). \quad (16)$$

Theorem 2: The exact analytical expression for outage probability of energy harvesting DF relay networks with the suboptimal TAS₁ scheme can be derived as

$$\begin{aligned}
 P_{\text{out}}^{\text{sub1}}(\gamma_{\text{th}}) & = \left[1 - \frac{1}{\Gamma(N_d)} \Gamma\left(N_d, \frac{\gamma_{\text{th}}}{\bar{\gamma}_0}\right) \right] \left[1 - \frac{N_s}{1-\alpha} \right. \\ & \times \frac{\gamma_{\text{th}}}{\bar{\gamma}_1} \sum_{n=0}^{N_s-1} \binom{N_s-1}{n} \sum_{m=0}^{N_d-1} \sum_{k=0}^{\infty} \frac{(-1)^{k+n}}{m!k!} \\ & \left. \times \left(\frac{1-\alpha}{\alpha \eta \Omega_2}\right)^{m+k} E_{m+k}\left(\frac{\gamma_{\text{th}}(n+1)}{(1-\alpha)\bar{\gamma}_1}\right) \right]. \quad (17)
 \end{aligned}$$

Proof: See Appendix C. ■

From Theorems 1 and 2, we can see that the difference of the outage probabilities achieved by optimal TAS scheme and suboptimal TAS₁ scheme lies in the first part of Eqs. (14) and (10), which is independent of the relaying link. This is due to that in the optimal TAS scheme, the selected antenna is the optimal to both the direct link and the relaying link, respectively.

Likewise, we now turn our attention to analyzing the asymptotic outage probability in the high SNR regime and we have the following key result.

Corollary 2: In the high SNR regime, i.e., $\bar{\gamma} \rightarrow \infty$, the outage probability of energy harvesting DF relay networks with the suboptimal TAS₁ scheme can be approximated as (18), as shown at the top of this page.

Proof: Similarly, as in the proof of Corollary 1, the above result can be easily obtained after some simple mathematical manipulations. ■

C. SUBOPTIMAL TAS₂ SCHEME

In this section, we focus on analyzing the outage performance of the considered system with the suboptimal TAS₂ scheme. As indicated in (8) and (11), the outage probability achieved

$$P_{\text{out}}^{\text{sub2}}(\gamma_{\text{th}}) \approx \begin{cases} \frac{1}{(N_d!)^{N_s}} \left(\frac{\gamma_{\text{th}}}{\bar{\gamma}_0}\right)^{N_s N_d} \frac{\gamma_{\text{th}}}{(1-\alpha)\bar{\gamma}_1} \left[1 + \frac{1}{\Gamma(N_d)} \sum_{k=0}^{\infty} \frac{(-1)^k \vartheta^{N_d+k}}{k! (N_d+k) (N_d+k-1)} \right], & N_d > 1 \\ \frac{1}{(N_d!)^{N_s}} \left(\frac{\gamma_{\text{th}}}{\bar{\gamma}_0}\right)^{N_s N_d} \frac{\gamma_{\text{th}}}{(1-\alpha)\bar{\gamma}_1} \left\{ 1 - \vartheta \left[\ln\left(\frac{\gamma_{\text{th}}}{(1-\alpha)\bar{\gamma}_1}\right) + \mathbf{C} \right] + \sum_{k=1}^{\infty} \frac{(-1)^k \vartheta^{k+1}}{(k+1)!k} \right\}, & N_d = 1 \end{cases} \quad (21)$$

$$P_{\text{out}}^{\text{delay}}(\gamma_{\text{th}}) = N_s \sum_{m=0}^{N_s-1} \binom{N_s-1}{m} \frac{(-1)^m \Phi}{(N_d-1)!} \sum_{k=0}^{\varphi} \binom{\varphi}{k} \frac{\Gamma(N_d+\varphi)}{\Gamma(N_d+k)} \frac{\rho_0^k (1-\rho_0)^{\varphi-k}}{\zeta^\varphi (1+m)^{N_d+k}} \Upsilon\left(N_d+k, \frac{1+m}{\zeta} \frac{\gamma_{\text{th}}}{\bar{\gamma}_0}\right) \times \left[1 - \frac{N_s \gamma_{\text{th}}}{(1-\alpha)\bar{\gamma}_1} \sum_{n=0}^{N_s-1} \binom{N_s-1}{n} \frac{(-1)^n}{\beta} \sum_{v=0}^{N_d-1} \frac{1}{v!} \sum_{k=0}^{\infty} \frac{(-1)^k}{k!} \left(\frac{1-\alpha}{\alpha\eta\Omega_2}\right)^{v+k} E_{v+k}\left(\frac{\gamma_{\text{th}}(n+1)}{(1-\alpha)\bar{\gamma}_1\beta}\right) \right]. \quad (24)$$

by the suboptimal TAS₂ scheme is given by

$$P_{\text{out}}^{\text{sub2}}(\gamma_{\text{th}}) = \Pr\left(\max_{1 \leq i \leq N_s} \gamma_{0,i} < \gamma_{\text{th}}\right) \Pr(\gamma_{\text{SR},i^*} < \gamma_{\text{th}}). \quad (19)$$

Theorem 3: The exact analytical expression for outage probability of energy harvesting DF relay networks with the suboptimal TAS₂ scheme can be derived as

$$P_{\text{out}}^{\text{sub2}}(\gamma_{\text{th}}) = \left[1 - \frac{1}{\Gamma(N_d)} \Gamma\left(N_d, \frac{\gamma_{\text{th}}}{\bar{\gamma}_0}\right) \right]^{N_s} \left[1 - \frac{\gamma_{\text{th}}}{1-\alpha} \times \frac{1}{\bar{\gamma}_1} \sum_{m=0}^{N_d-1} \sum_{k=0}^{\infty} \frac{(-1)^k}{m!k!} \left(\frac{1-\alpha}{\alpha\eta\Omega_2}\right)^{m+k} \times E_{m+k}\left(\frac{\gamma_{\text{th}}}{(1-\alpha)\bar{\gamma}_1}\right) \right]. \quad (20)$$

Proof: It is easily to obtain the above result by following similar steps as in Theorem 2. ■

Now, in the following, we turn our attention to analyze the outage probability of the suboptimal TAS₂ scheme in the high SNR regime, and we have the following key result.

Corollary 3: The outage probability of energy harvesting DF relay networks with the suboptimal TAS₂ scheme can be derived as (21), as shown at the top of this page, where **C** denotes the Euler’s constant [40, eq. (8.367.1)].

Proof: Similarly, as in the proof of Corollary 2, the above result can be easily obtained after some simple mathematical manipulations. ■

D. IMPACT OF FEEDBACK DELAY

In practice, the transmit antenna may be selected based on the outdated CSI due to feedback delay. Thus, in this section, the impact of feedback delay on the outage performance of optimal TAS scheme for energy harvesting DF relay networks is studied.²

Without loss of generality, we assume that the transmit antenna at *S* is selected based on the outdated CSIs of links *S* → *D* and *S* → *R*, which are feeded back from the receivers *R* and *D*, respectively. In order to make the subsequently

²Due to the space limitation, we only consider the impact of feedback delay on the optimal TAS scheme in this paper.

analysis tractable, we first model the CSIs of links *S* → *D* and *S* → *R* as follows:

$$h_{1,i} = \rho_1 \tilde{h}_{1,i} + \sqrt{(1-\rho_1^2)} e_1 \quad (22)$$

and

$$\mathbf{h}_{0,i} = \rho_0 \tilde{\mathbf{h}}_{0,i} + \sqrt{(1-\rho_0^2)} \mathbf{e}_0, \quad (23)$$

where $\tilde{h}_{1,i}$ and $\tilde{\mathbf{h}}_{0,i}$ denote the outdated CSIs between the *i*-th antenna at *S* and *R*, and the *i*-th antenna at *S* and *D*, respectively. ρ_1 and ρ_0 are the time correlation coefficients, which are defined as $\rho_i = \mathcal{J}_0(2\pi f_i \tau_i)$ with f_i being the maximum Doppler frequency and τ_i being the time delay of feedback, respectively. e_1 and \mathbf{e}_0 represent the error variables, which are utilized to quantify the correctness of feedback. Now, under this model, we present the outage performance of optimal TAS scheme with feedback delay in the following.

Theorem 4: The exact analytical expression for outage probability of energy harvesting DF relay networks with the optimal TAS scheme in the presence of feedback delay can be derived as (24), as shown at the top of this page, where $\Upsilon(\cdot, \cdot)$ is the lower incomplete Gamma function [40, eq. (8.350.1)], $\zeta = 1 + m(1 - \rho_0)$, $\beta = 1 + (1 - \rho_1)n$, and

$$\Phi = \sum_{m_1=0}^m \sum_{m_2=0}^{m_1} \cdots \sum_{m_{N_d-1}=0}^{m_{N_d-2}} \frac{m!}{m_{N_d-1}!} \prod_{t=1}^{N_d-1} \frac{(t!)^{m_{t+1}-m_t}}{(m_{t-1}-m_t)!} \quad (25)$$

with $m_0 = m, m_{N_d} = 0$, and $\varphi = \sum_{q=1}^{N_d-1} m_q$.

Proof: See Appendix D. ■

Following, we present the asymptotic outage probability of optimal TAS scheme to evaluate the impact of outdated CSI on the achievable diversity order and coding gain.

Corollary 4: The outage probability of energy harvesting DF relay networks with optimal TAS scheme in the presence of feedback delay can be derived as (26), as shown at the bottom of the next page.

Proof: By following similar steps to those in Appendix B, the asymptotic outage probability for the optimal TAS scheme in the presence of feedback delay can be easily obtained. ■

E. THE OPTIMAL POWER-SPLITTING RATIO

For the delay intolerant transmission, the source transmits at a constant rate $R_0 = \frac{1}{2} \log(1 + \gamma_{th})$, which may be subjected to outage due to fading. Hence the average throughput can be expressed as

$$R(\alpha) = (1 - P_{out}^*(\gamma_{th})) R_0, \tag{27}$$

where $\star \in \{\text{opt}, \text{sub1}, \text{sub2}, \text{delay}\}$. Now, by substituting Eq. (14), Eq. (17), Eq. (20) and (24) into Eq. (27), the average throughput achieved by the considered system with three TAS schemes can be easily evaluated.

On the other hand, having characterized the average throughput of the considered system, the optimal power-splitting α can be obtained by solving the following optimization problem.

$$\begin{aligned} \alpha^* &= \arg \max_{\alpha} R(\alpha) \\ \text{s.t. } &0 < \alpha < 1 \end{aligned} \tag{28}$$

In general, due to the complexity of the involved expression, obtaining an exact closed-form solution of α^* is very challenging. However, it can be efficiently solved by a one-dimensional search, or instead, it can be numerically evaluated using the build-in function ‘‘NSlove’’ of Mathematica.

V. NUMERICAL RESULTS

In this section, Monte Carlo simulations are provided to validate the analytical results and evaluate the impact of key parameters on the average throughput of the system. Unless otherwise specified, the following parameters are set: the power-splitting factor $\alpha = 0.5$, the energy conversion efficiency $\eta = 0.8$ and the outage threshold $\gamma_{th} = 1$. Similar to [42], the average channel power gains are modeled as $\Omega_0 = (1 + d_0^\tau)^{-1}$, $\Omega_1 = (1 + d_1^\tau)^{-1}$, and $\Omega_2 = (1 + d_2^\tau)^{-1}$, where d_0 , d_1 and d_2 are the distances between source and destination, source and relay, and relay and destination, respectively, τ denotes the path loss exponent. In addition, we set $d_0 = 5\text{m}$, $d_1 + d_2 = d_0$, and $\tau = 2$, respectively. As indicated in these figures, we can see that the analytical results are in good agreement with the simulation results and the asymptotic curves work quite well at high SNR regimes, which corroborates the accuracy of our derivation.

Figs. 2 and 3 show the impact of antenna numbers N_s and N_d on the outage probability of the considered system with three TAS schemes, respectively. As illustrated in these two figures, we can see that the outage performance of three TAS schemes can be improved by increasing N_s or N_d .

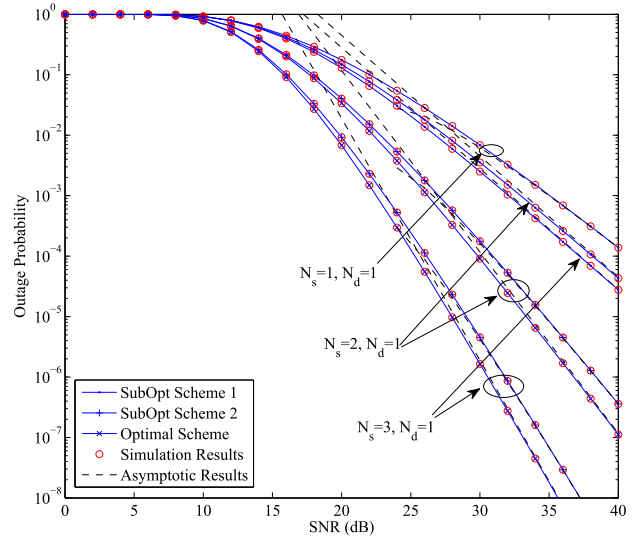


FIGURE 2. Outage probability of three TAS schemes with different N_s , $d_1 = 3\text{m}$ and $d_2 = 2\text{m}$.

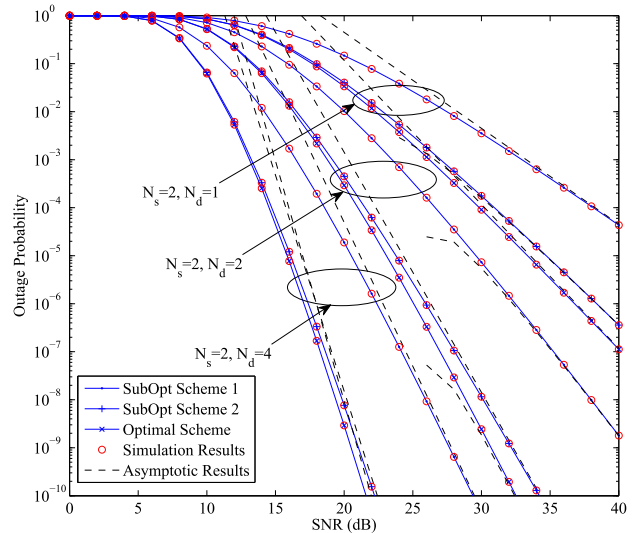


FIGURE 3. Outage probability of three TAS schemes with different N_d , $d_1 = 3\text{m}$ and $d_2 = 2\text{m}$.

However, different from the optimal TAS scheme and suboptimal TAS₂ scheme, increasing N_s produces a marginal impact on the outage performance of the suboptimal TAS₁ scheme. This is due to the fact that increasing N_s does not provide any additional diversity order to the suboptimal TAS₁ scheme. Contrarily, increasing N_d can significantly improve

$$\begin{aligned} &P_{out}^{\text{delay}}(\gamma_{th}) \\ &\approx \begin{cases} \frac{N_s^2 \gamma_{th}}{(1-\alpha) \bar{\gamma}_1} \left(\frac{\gamma_{th}}{\bar{\gamma}_0}\right)^{N_d} \sum_{m=0}^{N_s-1} \sum_{n=0}^{N_s-1} \binom{N_s-1}{m} \binom{N_s-1}{n} \frac{(-1)^{m+n} \Phi \Gamma(N_d + \varphi) (1-\rho_0)^\varphi}{\Gamma(N_d) \Gamma(N_d+1) \beta \zeta^{N_d+\varphi}} \left[1 + \frac{1}{\Gamma(N_d)} \sum_{k=0}^{\infty} \frac{(-1)^k \vartheta^{N_d+k}}{k! (N_d+k) (N_d+k-1)} \right], & \rho_1 \neq 1, N_d \neq 1 \\ \frac{N_s^2 \gamma_{th}}{(1-\alpha) \bar{\gamma}_1} \frac{\gamma_{th}}{\bar{\gamma}_0} \sum_{m=0}^{N_s-1} \sum_{n=0}^{N_s-1} \binom{N_s-1}{m} \binom{N_s-1}{n} \frac{(-1)^{m+n}}{\beta \zeta} \left\{ 1 - \vartheta \left[\ln\left(\frac{\varpi}{\beta}\right) + C \right] + \sum_{k=1}^{\infty} \frac{(-1)^k \vartheta^{k+1}}{k(k+1)!} \right\}, & \rho_1 \neq 1, N_d = 1 \end{cases} \end{aligned} \tag{26}$$

the outage performance of three TAS schemes due to the additional diversity order achieved by all three schemes as indicated in Corollaries 1-3. In addition, compared to the sub-optimal TAS₁ scheme, the suboptimal TAS₂ scheme achieves a similar performance as the optimal TAS scheme.

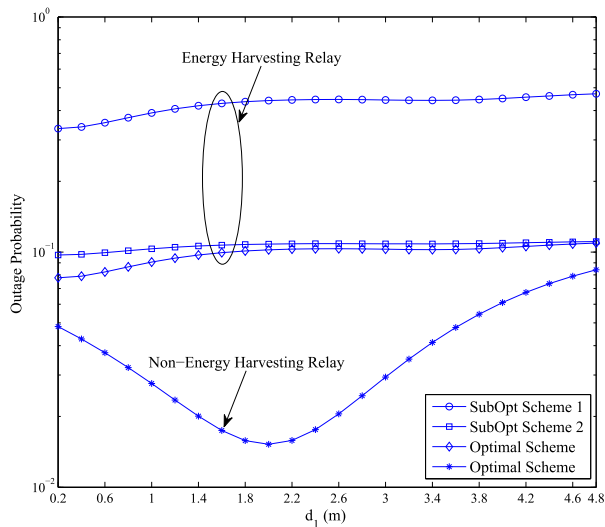


FIGURE 4. Impact of relay location on outage probability with $N_s = 3$, $N_d = 3$, $\bar{\gamma} = 10\text{dB}$ and $d_2 = 5 - d_1$.

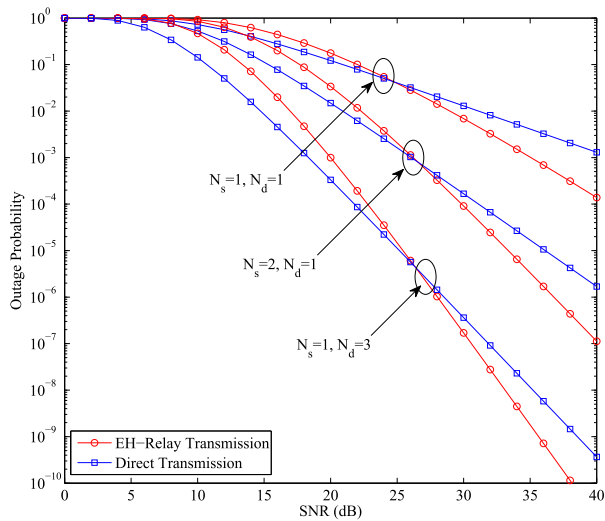


FIGURE 5. Outage probability comparison between EH-relay transmission and direct transmission with optimal TAS scheme with $d_1 = 3\text{m}$ and $d_2 = 2\text{m}$.

Fig. 4 investigates the impact of relay location on the outage probability of the system with three TAS schemes, respectively. As shown in the figure, we can see that different from the non-energy harvesting relay system, where the optimal relay location is almost in the middle of the source and the destination, while the optimal relay location for the energy harvesting relay system tends to be close to the source. Moreover, in Fig. 5, we make a comparison between the energy harvesting relay transmission and direct transmission,

where the maximal ratio combining is adopted to combine the received signals during the two slots in direct transmission. As shown in Fig. 5, we can see that the direct transmission has a better outage performance than that of the energy harvesting relay transmission at the low SNR regime, while the opposite holds in the high SNR regime. This is intuitive, increasing the transmit power at source can increase the harvesting energy at relay, which results in a larger transmit power at the relay during the second phase.

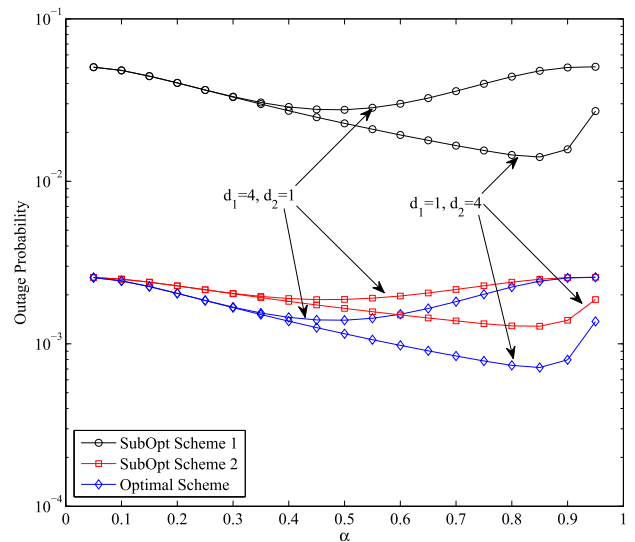


FIGURE 6. Outage probability versus the power-splitting ratio α with $N_s = 2$, $N_d = 3$ and $\bar{\gamma} = 15\text{dB}$.

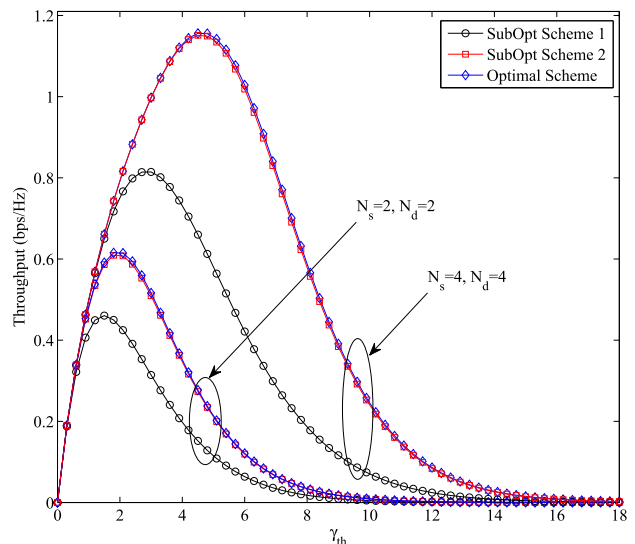


FIGURE 7. Impact of outage threshold on the throughput with $d_1 = 2\text{m}$, $d_2 = 3\text{m}$ and $\bar{\gamma} = 15\text{dB}$.

Figs. 6 and 7 examine the impacts of the power-splitting ratio and the outage threshold on the outage probability and the average throughput of the considered system, respectively. It is shown in Fig. 6 that there exists an optimal power-splitting ratio for all three TAS schemes as discussed in (28).

Moreover, when the relay is placed in closed to the source, the optimal power-splitting ratio will be increased due to the fact that since the relay is closed to the source, the quality of the second hop channel becomes the bottleneck in determining the performance of the relaying link. On the other hand, from Fig. 7, there also exist an optimal outage threshold for all three TAS schemes. This is intuitive, since according to (28), when the outage threshold is small, the transmit rate R_0 is small; when the outage threshold is large, the outage probability increases significantly, which again degrades the throughput. In addition, we find an interesting phenomenon that the optimal outage threshold is similar to the optimal scheme and the suboptimal TAS₂ scheme.

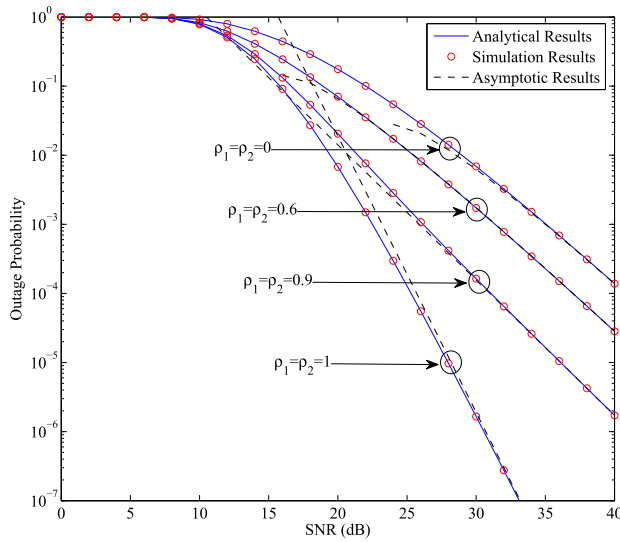


FIGURE 8. Impact of outdated CSI on outage probability of optimal antenna selection with $N_s = 3$, $N_d = 1$, $d_1 = 2m$ and $d_2 = 3m$.

Fig. 8 examines the impact of feedback delay on the outage probability of the considered system with optimal TAS scheme. It is shown in this figure, we can see that when there exists no feedback delay, i.e., $\rho_0 = \rho_1 = 1$, the full diversity order 4 can be achieved by the system. However, when $\rho_0 \neq 1$ and $\rho_1 \neq 1$, the diversity order achieved by the considered system will be reduced to 2 from the full diversity order 4, which indicates that the feedback delay has a severe detrimental effect on the outage probability.

VI. CONCLUSIONS

In this paper, we have proposed three TAS schemes for energy harvesting DF relay networks with power-splitting scheme based on the CSI of different links. Specifically, in order to evaluate the performance of the proposed three TAS schemes, the exact analytical expressions for the outage probability of the considered system were derived in non-identical Rayleigh fading channels. In addition, we also investigated the impact of feedback delay on the outage performance of optimal TAS scheme based on the derived analytical results. Moreover, to exploit useful design insights into the system, the asymptotic outage probabilities of the system with all the schemes

were provided, which enable us easily to obtain the diversity order and coding gain. The findings of this paper suggest that a) The diversity order obtained by the three TAS schemes is the same as the non-energy harvesting cooperative relay system; 2) The second suboptimal TAS schemes achieve a similar outage performance as the optimal TAS scheme with much lower implementation complexity; 3) The feedback delay has a significant negative impact on the diversity order of the considered system.

APPENDIX A PROOF OF THEOREM 1

In order to derive the outage probability of optimal TAS scheme, we first present the CDF of RV $Z = \min \{ (1 - \alpha), \alpha \eta \|\mathbf{h}_{RD}\|_F^2 \}$ as follows [25, Appendix B]:

$$F_Z(z) = \begin{cases} 1, & z > 1 - \alpha \\ \Pr \left(\|\mathbf{h}_{RD}\|^2 < \frac{z}{\alpha \eta} \right), & z < 1 - \alpha. \end{cases} \quad (29)$$

Since $\|\mathbf{h}_{RD}\|_F^2$ follows Chi-square distribution, we have

$$F_Z(z) = \begin{cases} 1, & z > 1 - \alpha \\ 1 - \frac{1}{\Gamma(N_d)} \Gamma \left(N_d, \frac{z}{\alpha \eta \Omega_2} \right), & z < 1 - \alpha. \end{cases} \quad (30)$$

Now, conditioned on Z , the outage probability in (13) can be rewritten as

$$\begin{aligned} P_{\text{out}}^{\text{opt}}(\gamma_{\text{th}}) &= E_Z \left[\Pr \left(\max \{ \gamma_{0,i^*}, \gamma_{\text{SR},i^*} \} < \gamma_{\text{th}} \right) \right] \\ &= E_Z \left[\left(\Pr(\gamma_{0,i} < \gamma_{\text{th}}) \Pr(\gamma_{\text{SR},i} < \gamma_{\text{th}}) \right)^{N_s} \right] \\ &= \left[\Pr(\gamma_{0,i} < \gamma_{\text{th}}) \right]^{N_s} E_Z \left[\left(\Pr(\gamma_{\text{SR},i} < \gamma_{\text{th}}) \right)^{N_s} \right], \end{aligned} \quad (31)$$

where $E_Z[\cdot]$ denotes the expectation operator with respect to the RV Z . Since $\|\mathbf{h}_{0,i}\|_F^2$ follows Chi-square distribution, we have

$$\Pr(\gamma_{0,i} < \gamma_{\text{th}}) = 1 - \frac{1}{\Gamma(N_d)} \Gamma \left(N_d, \frac{\gamma_{\text{th}}}{\bar{\gamma}_0} \right), \quad (32)$$

where $\bar{\gamma}_0 = \bar{\gamma} \Omega_0$.

On the other hand, according to (4), (6) and (7), we have

$$\begin{aligned} \Pr(\gamma_{\text{SR},i} < \gamma_{\text{th}}) &= \Pr \left(\bar{\gamma} |h_{1,i}|^2 z < \gamma_{\text{th}} \right) \\ &= 1 - \exp \left(-\frac{\gamma_{\text{th}}}{z \bar{\gamma}_1} \right). \end{aligned} \quad (33)$$

where $\bar{\gamma}_1 = \bar{\gamma} \Omega_1$. Now, with the help of (30), (33) and integration by parts, the expectation in (31) can be derived as (34), as shown at the top of the next page. To the best of our authors' knowledge, the integral in (34) does not admit a closed-form expression. Hence, in order to avoid the integral expression, we substitute the Maclaurin expansion

$$E_Z \left[\left(\Pr(\gamma_{SR,i} < \gamma_{th}) \right)^{N_s} \right] = 1 - \frac{N_s}{\Omega_1} \sum_{n=0}^{N_s-1} \binom{N_s-1}{n} (-1)^n \sum_{m=0}^{N_d-1} \frac{1}{m!} \left(\frac{\gamma_{th}}{\alpha \eta \Omega_2 \bar{\gamma}} \right)^m \times \int_{\frac{\gamma_{th}}{(1-\alpha)\bar{\gamma}}}^{\infty} \frac{1}{x^m} \exp\left(-\frac{\gamma_{th}}{\alpha \eta \Omega_2 \bar{\gamma} x}\right) \exp\left(-\frac{n+1}{\Omega_1} x\right) dx \quad (34)$$

$$E_Z \left[\left(\Pr(\gamma_{SR,i} < \gamma_{th}) \right)^{N_s} \right] \approx \left[\frac{\gamma_{th}}{(1-\alpha)\Omega_1\bar{\gamma}} \right]^{N_s} + \frac{N_s \gamma_{th}}{(1-\alpha)\Omega_1\bar{\gamma}} \times \sum_{n=0}^{N_s-1} \binom{N_s-1}{n} \frac{(-1)^n}{\Gamma(N_d)} \sum_{k=0}^{\infty} \frac{(-1)^k}{k! (N_d+k)} \left(\frac{1-\alpha}{\alpha \eta \Omega_2} \right)^{N_d+k} E_{N_d+k} \left(\frac{\gamma_{th}(n+1)}{(1-\alpha)\bar{\gamma}\Omega_1} \right) \quad (37)$$

$$E_Z \left[\left(\Pr(\gamma_{SR,i} < \gamma_{th}) \right)^{N_s} \right] \approx \left[\frac{\gamma_{th}}{(1-\alpha)\Omega_1\bar{\gamma}} \right]^{N_s} + \frac{N_s \gamma_{th}}{(1-\alpha)\Omega_1\bar{\gamma}} \sum_{n=0}^{N_s-1} \binom{N_s-1}{n} \frac{(-1)^n}{\Gamma(N_d)} \sum_{k=0}^{\infty} \frac{(-1)^k}{k! (N_d+k)} \times \left\{ \frac{(-\varpi)^{N_d+k-1}}{\Gamma(N_d+k)} [-\ln(\varpi) + \psi(N_d+k)] - \sum_{m=0, m \neq N_d+k-1}^{\infty} \frac{(-\varpi)^m}{(m-N_d-k+1)m!} \right\} \quad (38)$$

of the term $\exp\left(-\frac{u}{x}\right) = \sum_{k=0}^{\infty} \frac{(-1)^k}{k!} \left(\frac{u}{x}\right)^k$ into (34), and then we have

$$E_Z \left[\left(\Pr(\gamma_{SR,i} < \gamma_{th}) \right)^{N_s} \right] = 1 - \frac{N_s \gamma_{th}}{(1-\alpha)\Omega_1\bar{\gamma}} \sum_{n=0}^{N_s-1} \binom{N_s-1}{n} \times \sum_{m=0}^{N_d-1} \sum_{k=0}^{\infty} \frac{(-1)^{k+n}}{m!k!} \left(\frac{1-\alpha}{\alpha \eta \Omega_2} \right)^{m+k} E_{m+k} \left(\frac{\gamma_{th}(n+1)}{(1-\alpha)\bar{\gamma}\Omega_1} \right), \quad (35)$$

where we have used [41, eq. (5.1.4)] to solve the corresponding integral. To this end, the desired result in **Theorem 1** can be easily obtained after some simple mathematical manipulations.

**APPENDIX B
PROOF OF COROLLARY 1**

With the help of the series expansion of $\Gamma(\cdot, \cdot)$ [40, eq. (8.354.2)] and omitting the higher order terms, the approximation of (32) under $\bar{\gamma} \rightarrow \infty$ is given by

$$\Pr(\gamma_{0,i} < \gamma_{th}) \approx \frac{1}{N_d!} \left(\frac{\gamma_{th}}{\bar{\gamma}_0} \right)^{N_d}. \quad (36)$$

Similarly, applying the series expansion of $\Gamma(\cdot, \cdot)$ to (30), the approximation of (35) under $\bar{\gamma} \rightarrow \infty$ can be derived as (37), as shown at the top of this page. Now, by invoking [41, eq. (5.1.12)], the Eq. (37) can be further rewritten as (38), as shown at the top of this page.

Finally, by combining Eqs. (31), (36) and (38) together, the asymptotic outage probability of the system with optimal TAS scheme can be obtained after performing some mathematical manipulations.

**APPENDIX C
PROOF OF THEOREM 2**

Since the antenna selected at S only depends on the CSI of $S \rightarrow R$ link, hence the first term in (16) can be derived as follows:

$$\Pr(\gamma_{0,i^*} < \gamma_{th}) = 1 - \frac{1}{\Gamma(N_d)} \Gamma\left(N_d, \frac{\gamma_{th}}{\bar{\gamma}_0}\right). \quad (39)$$

On the other hand, the second term in (16) can be further expressed as

$$\Pr\left(\max_{1 \leq i \leq N_s} \gamma_{SR,i} < \gamma_{th}\right) = \Pr(\bar{\gamma} X Z < \gamma_{th}), \quad (40)$$

where $X = \max_{1 \leq i \leq N_s} |h_{1,i}|^2$, and the PDF of which is given by

$$f_X(x) = \frac{N_s}{\Omega_1} \sum_{n=0}^{N_s-1} \binom{N_s-1}{n} (-1)^n \exp\left(-\frac{n+1}{\Omega_1} x\right). \quad (41)$$

Further, by substituting the PDF of RV X and the CDF of RV Z into (41), we have

$$\Pr\left(\max_{1 \leq i \leq N_s} \gamma_{SR,i} < \gamma_{th}\right) = 1 - \frac{N_s}{\Omega_1} \sum_{n=0}^{N_s-1} \binom{N_s-1}{n} \times \frac{(-1)^n}{\Gamma(N_d)} \int_{\frac{\gamma_{th}}{(1-\alpha)\bar{\gamma}}}^{\infty} \Gamma\left(N_d, \frac{\gamma_{th}}{\alpha \eta \Omega_2 \bar{\gamma} x}\right) \exp\left(-\frac{n+1}{\Omega_1} x\right) dx. \quad (42)$$

Now, with the help of [40, eq. (8.352.7)] and [41, Eq. (5.1.4)], the analytical expression of (42) can be further simplified as the same to (37). To this end, by combining the above concerned equation, the desired outage probability in Theorem 2 can be easily obtained after some simple mathematical manipulations.

APPENDIX D

PROOF OF THEOREM 3

Let $\tilde{\gamma}_{0,i^*} = \bar{\gamma} \max_{1 \leq i \leq N_s} \|\tilde{\mathbf{h}}_{0,i}\|_F^2$ denote the τ_0 time-delayed version of γ_{0,i^*} , and $\tilde{\gamma}_{SR,i^*} = \bar{\gamma} \max_{1 \leq i \leq N_s} |\tilde{h}_{1,i}|^2$ denote the τ_1 time-delayed version of γ_{SR,i^*} . Hence, the outage probability achieved by the optimal TAS scheme in the presence of feedback delay is given by

$$P_{\text{out}}^{\text{delay}}(\gamma_{\text{th}}) = \Pr(\tilde{\gamma}_{0,i^*} < \gamma_{\text{th}}) \Pr(\tilde{\gamma}_{SR,i^*} < \gamma_{\text{th}}). \quad (43)$$

In order to solve the above equation, we first present the statistic of RVs $X_0 = \max_{1 \leq i \leq N_s} \|\mathbf{h}_{0,i}\|_F^2$ and $X_1 = \max_{1 \leq i \leq N_s} |\tilde{h}_{1,i}|^2$ as follows [43]:

$$F_{X_0}(x) = N_s \sum_{m=0}^{N_s-1} \binom{N_s-1}{m} \frac{(-1)^m \Phi}{(N_d-1)!} \sum_{k=0}^{\varphi} \binom{\varphi}{k} \times \frac{\Gamma(N_d+\varphi) \rho_0^k (1-\rho_0)^{\varphi-k}}{\Gamma(N_d+k) \zeta^\varphi (1+m)^{N_d+k}} \Upsilon\left(N_d+k, \frac{1+m}{\zeta \Omega_0} x\right) \quad (44)$$

and

$$f_{X_1}(x) = \frac{N_s}{\Omega_1} \sum_{n=0}^{N_s-1} \binom{N_s-1}{n} \frac{(-1)^n}{\beta} \exp\left(-\frac{n+1}{\beta \Omega_1} x\right). \quad (45)$$

Now, by following similar analysis in Appendix C, the desired result can be easily derived after performing some mathematical manipulations.

REFERENCES

[1] V. Raghunathan, S. Ganeriwal, and M. Srivastava, "Emerging techniques for long lived wireless sensor networks," *IEEE Commun. Mag.*, vol. 44, no. 4, pp. 108–114, Apr. 2006.

[2] S. Sudevalayam and P. Kulkarni, "Energy harvesting sensor nodes: Survey and implications," *IEEE Commun. Surveys Tuts.*, vol. 13, no. 3, pp. 443–461, 3rd Quart., 2011.

[3] W. Lumpkins, "Nikola Tesla's dream realized: Wireless power energy harvesting," *IEEE Consum. Electron. Mag.*, vol. 3, no. 1, pp. 39–42, Jan. 2014.

[4] L. Xiao, P. Wang, D. Niyato, D. I. Kim, and Z. Han, "Wireless networks with RF energy harvesting: A contemporary survey," *IEEE Commun. Surveys Tuts.*, vol. 17, no. 2, pp. 757–789, 2nd Quart., 2014.

[5] L. R. Varshney, "Transporting information and energy simultaneously," in *Proc. IEEE Int. Symp. Inf. Theory (ISIT)*, Toronto, ON, Canada, Jul. 2008, pp. 1612–1616.

[6] P. Grover and A. Sahai, "Shannon meets tesla: Wireless information and power transfer," in *Proc. IEEE Int. Symp. Inf. Theory (ISIT)*, Austin, TX, USA, Jun. 2010, pp. 2363–2367.

[7] X. Zhou, R. Zhang, and C. Ho, "Wireless information and power transfer: Architecture design and rate-energy tradeoff," *IEEE Trans. Commun.*, vol. 61, no. 11, pp. 4757–4767, Nov. 2013.

[8] L. Liu, R. Zhang, and K.-C. Chua, "Wireless information transfer with opportunistic energy harvesting," *IEEE Trans. Wireless Commun.*, vol. 12, no. 1, pp. 288–300, Jan. 2013.

[9] C. Zhong, X. Chen, Z. Zhang, and G. K. Karagiannidis, "Wireless-powered communications: Performance analysis and optimization," *IEEE Trans. Commun.*, vol. 63, no. 12, pp. 5178–5190, Dec. 2015.

[10] L. Liu, R. Zhang, and K.-C. Chua, "Wireless information and power transfer: A dynamic power splitting approach," *IEEE Trans. Commun.*, vol. 61, no. 9, pp. 3990–4001, Sep. 2013.

[11] Z. Ding et al., "Application of smart antenna technologies in simultaneous wireless information and power transfer," *IEEE Commun. Mag.*, vol. 53, no. 4, pp. 86–93, Apr. 2015.

[12] X. Chen, Z. Zhang, H.-H. Chen, and H. Zhang, "Enhancing wireless information and power transfer by exploiting multi-antenna techniques," *IEEE Commun. Mag.*, vol. 53, no. 4, pp. 133–141, Apr. 2015.

[13] I. Krikidis, S. Timotheou, S. Nikolaou, G. Zheng, D. W. K. Ng, and R. Schober, "Simultaneous wireless information and power transfer in modern communication systems," *IEEE Commun. Mag.*, vol. 52, no. 11, pp. 104–110, Nov. 2014.

[14] R. Zhang and C. K. Ho, "MIMO broadcasting for simultaneous wireless information and power transfer," *IEEE Trans. Wireless Commun.*, vol. 12, no. 5, pp. 1989–2001, May 2013.

[15] S. Timotheou, I. Krikidis, G. Zheng, and B. Ottersten, "Beamforming for MISO interference channels with QoS and RF energy transfer," *IEEE Trans. Wireless Commun.*, vol. 13, no. 5, pp. 2646–2658, May 2014.

[16] W. Huang, H. Chen, Y. Li, and B. Vucetic, "On the performance of multi-antenna wireless-powered communications with energy beamforming," *IEEE Trans. Veh. Technol.*, vol. 65, no. 3, pp. 1801–1808, Mar. 2016.

[17] H. Lee, S.-R. Lee, K.-J. Lee, H.-B. Kong, and I. Lee, "Optimal beamforming designs for simultaneous wireless information and power transfer in MISO interference channels," *IEEE Trans. Wireless Commun.*, vol. 14, no. 9, pp. 3817–3822, Sep. 2015.

[18] G. Yang, C. K. Ho, R. Zhang, and Y. L. Guan, "Throughput optimization for massive MIMO systems powered by wireless energy transfer," *IEEE J. Sel. Areas Commun.*, vol. 33, no. 8, pp. 1640–1650, Aug. 2015.

[19] A. A. Nasir, X. Zhou, S. Durrani, and R. A. Kennedy, "Relaying protocols for wireless energy harvesting and information processing," *IEEE Trans. Wireless Commun.*, vol. 12, no. 7, pp. 3622–3636, Jul. 2013.

[20] A. A. Nasir, X. Zhou, S. Durrani, and R. A. Kennedy, "Wireless-powered relays in cooperative communications: Time-switching relaying protocols and throughput analysis," *IEEE Trans. Commun.*, vol. 63, no. 5, pp. 1607–1622, May 2015.

[21] Y. Gu and S. Aissa, "RF-based energy harvesting in decode-and-forward relaying systems: Ergodic and outage capacities," *IEEE Trans. Wireless Commun.*, vol. 14, no. 11, pp. 6425–6434, Nov. 2015.

[22] D. S. Michalopoulos, H. A. Suraweera, and R. Schober, "Relay selection for simultaneous information transmission and wireless energy transfer: A tradeoff perspective," *IEEE J. Sel. Areas Commun.*, vol. 33, no. 8, pp. 1578–1594, Aug. 2015.

[23] H. Ding, D. B. da Costa, X. Wang, U. S. Dias, R. T. de Sousa, and J. Ge, "On the effects of LOS path and opportunistic scheduling in energy harvesting relay systems," *IEEE Trans. Wireless Commun.*, vol. 15, no. 12, pp. 8506–8524, Dec. 2016.

[24] N. T. Do, D. B. da Costa, T. Q. Duong, V. N. Q. Bao, and B. An, "Exploiting direct links in multiuser multirelay SWIPT cooperative networks with opportunistic scheduling," *IEEE Trans. Wireless Commun.*, vol. 16, no. 8, pp. 5410–5427, Aug. 2017.

[25] G. Zhu, C. Zhong, H. A. Suraweera, G. K. Karagiannidis, Z. Zhang, and T. A. Tsiftsis, "Wireless information and power transfer in relay systems with multiple antennas and interference," *IEEE Trans. Commun.*, vol. 63, no. 4, pp. 1400–1418, Apr. 2015.

[26] Z. Zhou, M. Peng, Z. Zhao, and Y. Li, "Joint power splitting and antenna selection in energy harvesting relay channels," *IEEE Signal Process. Lett.*, vol. 22, no. 7, pp. 823–827, Jul. 2015.

[27] J. Men, J. Ge, and C. Zhang, "A joint relay-and-antenna selection scheme in energy-harvesting MIMO relay networks," *IEEE Signal Process. Lett.*, vol. 23, no. 4, pp. 532–536, Apr. 2016.

[28] M. Mohammadi, B. K. Chalise, H. A. Suraweera, C. Zhong, G. Zheng, and I. Krikidis, "Throughput analysis and optimization of wireless-powered multiple antenna full-duplex relay systems," *IEEE Trans. Commun.*, vol. 64, no. 4, pp. 1769–1785, Apr. 2016.

[29] A. Almradi and K. A. Hamdi, "The performance of wireless powered MIMO relaying with energy beamforming," *IEEE Trans. Commun.*, vol. 64, no. 11, pp. 4550–4562, Nov. 2016.

[30] L. Liu, J. C. Zhang, Y. Yi, H. Li, and Z. Zhang, "Combating interference: MU-MIMO, CoMP, and HetNet," *J. Commun.*, vol. 7, no. 9, pp. 646–655, 2012.

[31] D. B. D. Costa and S. Aissa, "Cooperative dual-hop relaying systems with beamforming over Nakagami- m fading channels," *IEEE Trans. Wireless Commun.*, vol. 8, no. 8, pp. 3950–3954, Aug. 2009.

[32] N. Yang, P. L. Yeoh, M. Elkashlan, I. B. Collings, and Z. Chen, "Two-way relaying with multi-antenna sources: Beamforming and antenna selection," *IEEE Trans. Veh. Technol.*, vol. 61, no. 9, pp. 3996–4008, Nov. 2012.

[33] S. Modem and S. Prakriya, "Performance of analog network coding based two-way EH relay with beamforming," *IEEE Trans. Commun.*, vol. 65, no. 4, pp. 1518–1535, Apr. 2017.

[34] G. Amarasuriya, C. Tellambura, and M. Ardakani, "Performance analysis framework for transmit antenna selection strategies of cooperative MIMO AF relay networks," *IEEE Trans. Veh. Technol.*, vol. 60, no. 7, pp. 3030–3044, Sep. 2011.

[35] Z. Ding, S. M. Perlaza, I. Esnaola, and H. V. Poor, "Power allocation strategies in energy harvesting wireless cooperative networks," *IEEE Trans. Wireless Commun.*, vol. 13, no. 2, pp. 846–860, Feb. 2014.

[36] K. M. Rabie, B. Adebisi, and M.-S. Alouini, "Half-duplex and full-duplex AF and DF relaying with energy-harvesting in log-normal fading," *IEEE Trans. Green Commun. Netw.*, vol. 1, no. 4, pp. 468–480, Dec. 2017.

[37] D. C. González, D. B. da Costa, and J. C. S. S. Filho, "Distributed suboptimal schemes for TAS/SC and TAS/LS in fixed-gain AF relaying systems," *IEEE Trans. Wireless Commun.*, vol. 13, no. 11, pp. 6041–6053, Nov. 2014.

[38] V. S. Krishna and M. R. Bhatnagar, "A joint antenna and path selection technique in single-relay-based DF cooperative MIMO networks," *IEEE Trans. Veh. Technol.*, vol. 65, no. 3, pp. 1340–1353, Mar. 2016.

[39] L. Cao, X. Zhang, Y. Wang, and D. Yang, "Transmit antenna selection strategy in amplify-and-forward MIMO relaying," in *Proc. IEEE Wireless Commun. Netw. Conf.*, Budapest, Hungary, Apr. 2009, pp. 1–4.

[40] I. S. Gradshteyn and I. M. Ryzhik, *Table of Integrals, Series, and Products*, 7th ed. San Diego, CA, USA: Academic, 2007.

[41] M. Abramowitz and I. A. Stegun, *Handbook of Mathematical Functions: With Formulas, Graphs, and Mathematical Tables*, 9th ed. New York, NY, USA: Dover, 1970.

[42] I. Krikidis, "Relay selection in wireless powered cooperative networks with energy storage," *IEEE J. Sel. Areas Commun.*, vol. 33, no. 12, pp. 2596–2610, Dec. 2015.

[43] Y. Huang, F. Al-Qahtani, C. Zhong, Q. Wu, J. Wang, and H. Alnuweiri, "Performance analysis of multiuser multiple antenna relaying networks with co-channel interference and feedback delay," *IEEE Trans. Commun.*, vol. 62, no. 1, pp. 59–73, Jan. 2014.



JINLONG WANG (SM'13) received the B.S. degree in mobile communications, and the M.S. and Ph.D. degrees in communications engineering and information systems from the Institute of Communications Engineering, Nanjing, China, in 1983, 1986, and 1992, respectively. He is currently a Professor with the College of Communications Engineering, Army Engineering University of PLA. He has published over 200 papers in refereed mainstream journals and reputed international conferences and has been granted over 20 patents in his research areas. His current research interests are the broad area of digital communications systems with emphasis on cooperative communication, adaptive modulation, multiple-input-multiple-output systems, soft-defined radio, cognitive radio, green wireless communications, and game theory.

Dr. Wang also has served as the Founding Chair and the Publication Chair of the International Conference on Wireless Communications and Signal Processing (WCSP) 2009, a member of the Steering Committees of WCSP 2010–2012, a TPC Member for several international conferences and a Reviewer for many famous journals. He is currently the Vice-Chair of the IEEE Communications Society Nanjing Chapter.



PING ZHANG (SM'15) received the B.S. and M.S. degrees in physics and electrical engineering from Northwest University, Xi'an, China, in 1982 and 1986, respectively, and the Ph.D. degree in electric circuits and systems from the Beijing University of Posts and Telecommunications (BUPT), Beijing, China, in 1990. From 1994 to 1995, he was a Post-Doctoral Researcher with the PCS Department, Korea Telecom Wireless System Development Center. He is currently a Professor with the School of Information and Communication Engineering, BUPT.

His research interests include key techniques of 3G and B3G systems, cognitive radio technology, cognitive wireless networks, and MIMO-OFDM. He was a recipient of the First and Second Prizes of the National Technology Invention and Technological Progress Awards and the First Prize of the Outstanding Achievement Award of Scientific Research in College. He is the Executive Associate Editor-in-Chief on Information Sciences of the *Chinese Science Bulletin*, a Guest Editor of the *IEEE Wireless Communications Magazine*, and an Editor of *China Communications*.



YUZHEN HUANG (S'12–M'16) received the B.S. degree in communications engineering and the Ph.D. degree in communications and information systems from the College of Communications Engineering, PLA University of Science and Technology, in 2008 and 2013, respectively. He is currently an Assistant Professor with the College of Communications Engineering, Army Engineering University of PLA. He has published nearly 70 research papers in international journals.

His research interests include channel coding, MIMO systems, cooperative communications, physical layer security, and cognitive radio systems. He received the Best Paper Award at WCSP 2013. He received an IEEE COMMUNICATIONS LETTERS Exemplary Reviewer Certificate in 2014. He served as an Associate Editor for the *KSII Transactions on Internet and Information Systems*.



QIHUI WU (SM'12) received the B.S. degree in communications engineering, and the M.S. and Ph.D. degrees in communications and information system from the Institute of Communications Engineering, Nanjing, China, in 1994, 1997, and 2000, respectively. He is currently a Professor with the College of Electronic and Information Engineering, Nanjing University of Aeronautics and Astronautics. His current research interests are algorithms and optimization for cognitive wireless networks, soft-defined radio, and wireless communication systems.

...